J. Physiol. (1984), **350**, *pp.* 401–412
With 9 text-figures
Printed in Great Britain

DIFFERENT QUANTAL RESPONSES WITHIN SINGLE FROG NEUROMUSCULAR JUNCTIONS

BY A. BIESER, A. WERNIG AND H. ZUCKER*
From the Department of Physiology, University of Bonn, D-5300 Bonn 1, F.R.G.

(*Received 17 May 1983*)

SUMMARY

1. At frog neuromuscular junctions spontaneous miniature end-plate potentials (m.e.p.p.s) were recorded from several isolated spots within single synapses. This was done by consecutively placing an extracellular glass micro-electrode (focal electrode) at different recording sites, while the intracellular electrode remained in one place.

2. After each set of recordings, muscles were stained to reveal both axon terminals and cholinesterase (ChE) such that the exact position of each recording site could be determined.

3. In many nerve terminal branches a similar quantum size was found at several different spots. In other instances, however, mean quantum amplitudes varied by 10–60 % at different spots along the same terminal branches.

4. As a control, individual spots were recorded from repeatedly after repositioning the focal electrode. In these recordings mean m.e.p.p. amplitude varied by only 5–10 %.

5. It is concluded that quantum size within a single junction is similar at many spots, but deviates markedly at others. Correlation of this variation with the stained preparations suggested that spots where quanta significantly larger or smaller than normal were recorded were either at ChE rings or at the distal ends of nerve branches, respectively; at different nerve terminal branches within the same junction, quantum amplitudes were similar in many cases but deviated in others.

6. The results are consistent with ultrastructural evidence that frog neuromuscular junctions are non-homogeneous structures which undergo continual remodelling.

INTRODUCTION

Evidence has been presented in previous investigations that the adult frog neuromuscular junction is not a static structure but continually undergoes some physiological remodelling (Wernig, Pécot-Dechavassine & Stöver, 1980*a*, *b*). In the preceding paper (Anzil, Bieser & Wernig, 1984), newly formed synaptic contacts were ascribed to sites which, in the light microscope appeared as small rings of cholinesterase (ChE) reaction product. Here we report electrophysiological data on spontaneous transmitter release at different points along a single neuromuscular junction. Experiments were performed by simultaneously recording spontaneous quantal discharges with an intracellular and an extracellular micro-electrode. During the

* Max-Planck-Institute for Psychiatry, D-8000 München 40, F.R.G.

experiment the extracellular (focal) electrode was moved to several different spots along the junction while the intracellular electrode remained stationary. The morphology of these spots was subsequently examined in stained whole-mount preparations.

Preliminary reports of this work have been published elsewhere (Bieser & Wernig, 1982).

METHODS

Animals

Experiments were performed on cutaneous pectoris muscles from normal adult frogs (*Rana temporaria*). All animals measured between 5·5 and 6·4 cm and weighed from 12 to 28 g. Most experiments were performed between October and April. The animals were kept in running water at 16 °C and fed twice a week.

Electrophysiology

Muscles were bathed in normal Ringer solution of the following composition (mM): 115, NaCl; 2·5, KCl; 1·8, $CaCl_2$; 2·15, Na_2HPO_4; 0·85, NaH_2PO_4; titrated to pH 7·2 at room temperature (20–22 °C). Miniature end-plate potentials (m.e.p.p.s) were sampled from different spots within single neuromuscular junctions by simultaneous recording with an extra- and an intracellular glass micro-electrode against a reference electrode in the bath. The intracellular electrode remained in the same position while the extracellular (focal) electrode (outer tip diameter ~ 4 μm) was moved to different spots along the same terminal. About 100–200 m.e.p.p.s were collected at each site. The same focal electrode was used throughout an experiment. As the end-plate current density decays steeply in the extracellular space, the focal electrode measured only those signals originating within a maximum distance of about 20–25 μm to each side along the nerve; these values were derived from a few experiments in which we determined the maximum distance at which one focal electrode recorded quantal discharges originating under a second focal electrode (discharges which gave the maximum amplitude signals in this electrode, cf. Wernig, 1976). These measurements were made on nerve terminal branches with apparently continuous synaptic contacts (as judged from the continuous double lines of ChE reaction product). We expect, however, that the extracellular length constant is much shorter at parts of nerve terminal branches with small, isolated synaptic contacts (e.g. ChE rings), since the cleft between the muscle fibre and the Schwann cell is considerably larger outside the immediate synaptic contact (see below and Anzil *et al.* 1984). Differences in the extracellular length constant should also arise from differences in the width of the synaptic gutter, which is bound to be different at terminal branches with different axon diameters (cf. Wernig *et al.* 1980*a*, *b*). Extra- and intracellular signals which appeared simultaneously were collected and analysed with a PDP 8 computer; mean m.e.p.p. amplitudes were calculated for each set of recordings.

Mean m.e.p.p. amplitudes obtained from a single neuromuscular junction were corrected for a common resting potential by weighting with the factor V_S/V_R, where V_S = the assumed common membrane potential and V_R = the actual resting potential during the sampling period. Correction for non-linear summation (Martin, 1955; McLachlan & Martin, 1981) was negligible and was thus omitted. Only experiments in which the drift in resting potential was less than 10 mV throughout were used for further evaluation.

Histochemical procedures

During electrophysiological examination, the morphological features which could be easily detected under Nomarski interference contrast optics (40 × water immersion) were drawn to scale with help of an eye-piece micrometer. After these measurements, the pinned-out muscle was fixed in the recording chamber and stained using a combined axon and ChE protocol (Pécot-Dechavassine, Wernig & Stöver, 1979). Consequently, recording sites were carefully located in the stained preparation. The staining procedure did not appear to affect muscle fibre length.

RESULTS

As shown in the preceding paper (Anzil *et al.* 1984), the morphological appearance of neuromuscular junctions is non-homogeneous. There are signs of nerve retraction (i.e. ChE remnants, asterisks in Fig. 1) and signs of possible new synapse formation (ChE rings, e.g. at positions 1 and 3/4, Fig. 1). It was the aim of the present investigation to gain information on spontaneous transmitter discharge at synaptic contacts that appeared to be newly formed. Fig. 1 illustrates the experimental situation and shows the results of a typical measurement. The upper part shows a

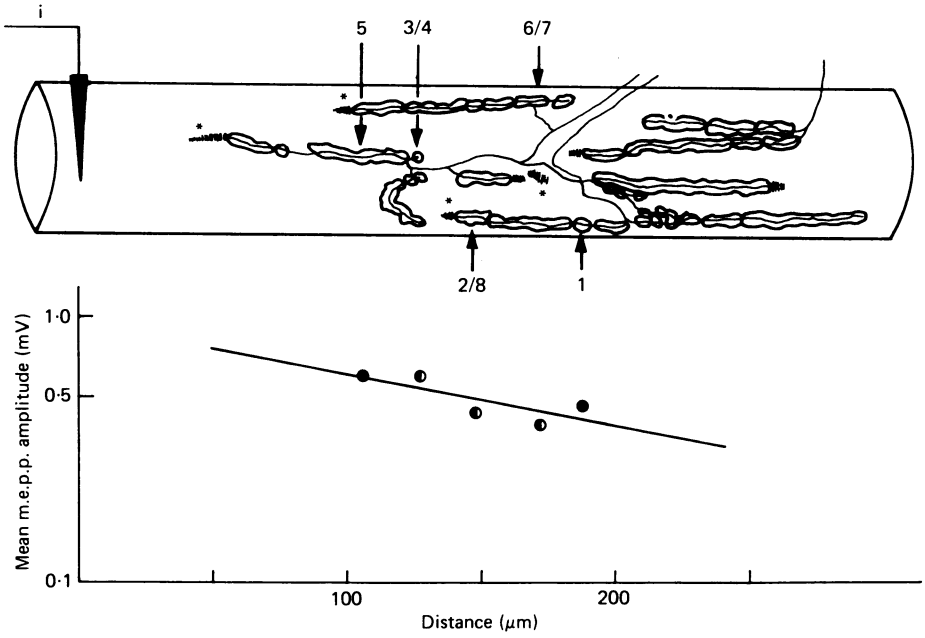

Fig. 1. Camera lucida drawing of a frog neuromuscular junction after a combined axon and ChE staining. The double lines represent the ChE reaction product, the inner lines the axon terminals. The position of the intracellular electrode is indicated by i. The arrows indicate the different focal electrode positions and the numbers (1–8), the sequence of recordings. In the lower part of the Figure, a semilogarithmic plot of the average m.e.p.p. amplitudes against distance between the intra- and extracellular electrodes is shown. The regression line and the corresponding length constant were calculated. The inner three spots were tested twice at different times during the experiment; the corresponding mean amplitudes are almost identical (◐). Also visible are ChE remnants (*) which most likely represent abandoned former synaptic sites (see preceding paper, Anzil *et al.* 1984).

camera lucida drawing of the junction under investigation after combined staining of the axon and ChE. The inner line in each branch represents the axon and the outer ones the ChE reaction product (see Pécot-Dechavassine *et al.* 1979; Wernig *et al.* 1980*a*, *b*). The arrows indicate the different positions of the focal electrode, the numbers 1–8 indicate the sequence of recordings. The inner three spots (3/4, 2/8, 6/7) were approached a second time after different intervals. The arrow to the left marks the position of the intracellular electrode (i). In the lower part of Fig. 1, the mean m.e.p.p. amplitudes are plotted against distance between the intra- and extracellular

electrodes. The comparable mean m.e.p.p. amplitudes from the double measurements are practically identical (half-filled circle for the inner three spots); this indicates that the sampling technique does not introduce large errors when evaluating the mean quantum amplitude at a given site (see below). Included in the plot is the calculated regression line which, however, gives a poor fit. All values should fall on a single straight line if quantum size were the same at all spots. This clearly is not the case in the experiment illustrated in Fig. 1. In thirty experiments performed in this way a reasonable fit was found only in nine synapses. In four experiments the regression lines had positive slopes and in two experiments the slopes were such that a length constant was obtained which seems unrealistic under the experimental conditions (3·4 mm and 16 mm) (see below).

Control measurements

To test the reliability of these measurements, we performed the following control experiments (see Discussion). First, multiple recordings were made from a single spot by repeatedly approaching the same spot with the focal electrode. In one set of experiments the focal pipette was reapplied as accurately as possible to the original site (filled bars in Fig. 2: upper histogram). In other experiments, the position of the

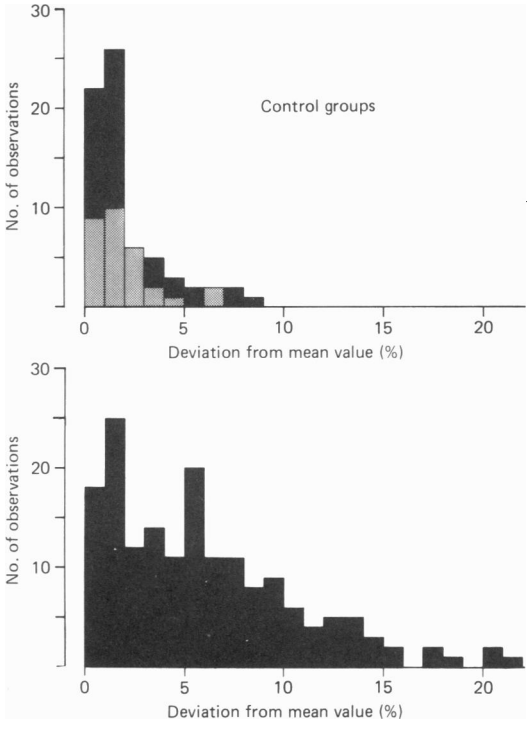

Fig. 2. Upper histogram: relative deviations from the mean values obtained after multiple measurements at one spot. Stippled columns: deviations after moving the focal electrode 1–2 μm from the original spot. Filled columns: deviations when trying to hit the identical spot. Lower histogram: relative deviations from calculated regression lines. Six experiments in which the regression line had a positive slope or gave an unrealistic length constant are not represented here.

focal electrode was purposefully shifted along the terminal by 1–2 μm on either side of the original spot (stippled bars). The values for the mean m.e.p.p. amplitude obtained from one spot were then compared. Fig. 2 (upper histogram) shows the scatter obtained from ninety-seven recordings at twenty-eight spots. The scatter is expressed as relative deviation of a value from the over-all mean amplitude calculated for one spot (i.e. average from all mean m.e.p.p. amplitudes). Usually three series of recordings (two to seven) were performed at an individual spot. In each recording 100–200 m.e.p.p.s were collected. As can be seen from the histogram, most values obtained by this procedure deviated by less than 5% from the means. This scatter can tentatively be compared with the relative deviations of individual points from the common regression line obtained from recordings at different points (cf. Fig. 1).

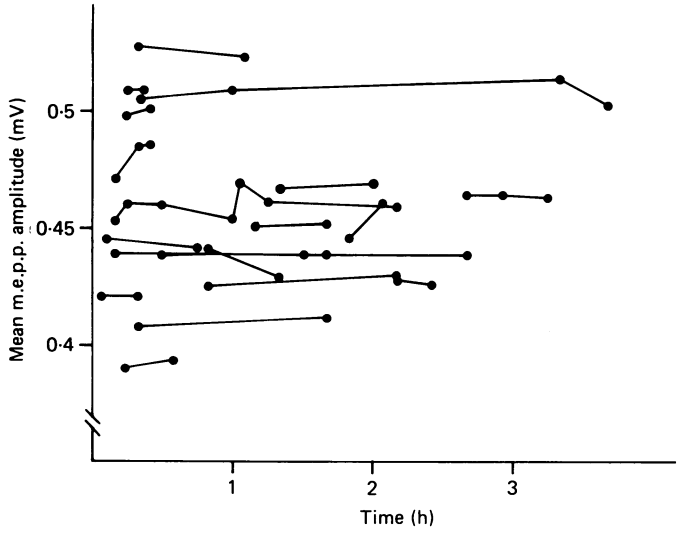

Fig. 3. Measurements at identical spots were performed repeatedly after different periods of time. Mean m.e.p.p. amplitudes are plotted against interval from the onset of the experiment; corresponding points are connected by lines.

The lower half of Fig. 2 shows such results from 170 spots in twenty-four synapses. Values from the six experiments which had a positive regression line or unrealistic length constants are not included in the graph.

To control for temporal effects, mean m.e.p.p. amplitudes obtained from identical spots were plotted against the time of recording after onset of the experiment. Fig. 3 shows forty-eight mean m.e.p.p. amplitudes obtained from eighteen spots. Corresponding points are connected by lines. No consistent change in the quantum size during the course of an experiment was observed, even over several hours.

The much larger scatter in the lower histogram of Fig. 2 compared to the control group (upper histogram in Fig. 2) suggests that the poor correlation found between mean m.e.p.p. amplitude and distance from the recording electrode is real. We conclude, therefore, that quantum size is not the same at all spots within a neuromuscular junction.

Correlation of amplitude deviations with terminal morphology

In the following we have analysed the morphology of the recording sites on stained muscles and looked for correlations between anatomical appearance and quantum amplitude. The neuromuscular junction illustrated in Fig. 4 contains four ChE rings, two of which were examined electrophysiologically (positions 1 and 6). Mean m.e.p.p. amplitudes obtained at the single spots were widely scattered around the regression

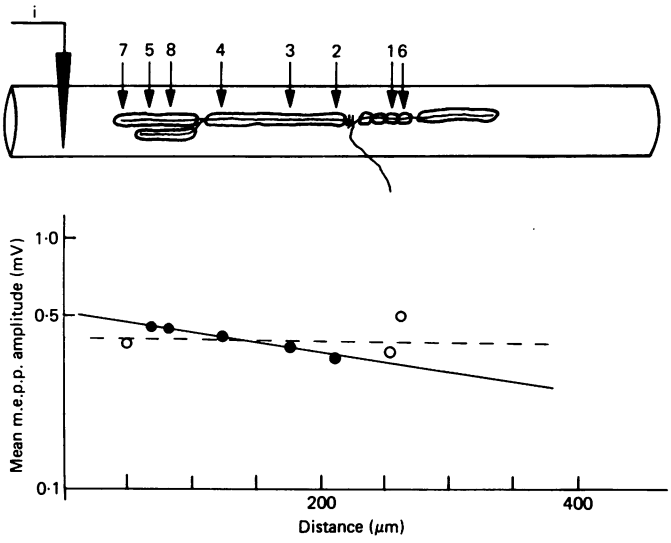

Fig. 4. Camera lucida drawing of a frog neuromuscular junction after a combined axon and ChE staining. Positions of the focal electrode are marked by arrows; the numbers give the time sequence of recordings. Intracellular electrode at i. Cell diameter 53 μm. Below: semilogarithmic plot of mean m.e.p.p. amplitudes *versus* distance between electrodes. Dashed line is the over-all regression line; continuous line is the regression line after eliminating three recordings (○) at the ChE rings (1, 6) and the distal nerve end (7).

line (dashed line; regression coefficient $r = -0{\cdot}188$). Using these data, the value for the length constant of this fibre (fibre diameter 53 μm) would be 3380 μm. Evidently, neither the regression coefficient nor the calculated length constant are meaningful. In considering the possible causes of these deviations, we noticed that three of the eight recording sites were located either at ChE rings or the distal ends of nerve branches (spots 1, 6 and 7, open circles in Fig. 4). Consequently, these points were eliminated. The new regression line (continuous) has a regression coefficient of $r = -0{\cdot}99$ and gives a length constant of 550 μm (a reasonable value for a fibre of this diameter, cf. Gage & McBurney, 1972; see below). The eliminated points deviate from the new regression line by 17 % (spot 1), 58 % (spot 6) and 10·9 % (spot 7), whereas the other points deviate by only 0·2–1·6 %.

In the experiment shown in Fig. 5, recordings were made from five different spots located on two different nerve branches. As above, the value obtained from the distal nerve terminal (spot 3) deviated markedly and was excluded from the calculation of the regression line. The other spots, though located at different collateral branches, had the same quantum size. Such correspondence, however, was not present in all synapses. In Fig. 6, spots 1/5, 2 and 3 (and spot 4) have the same quantum size while

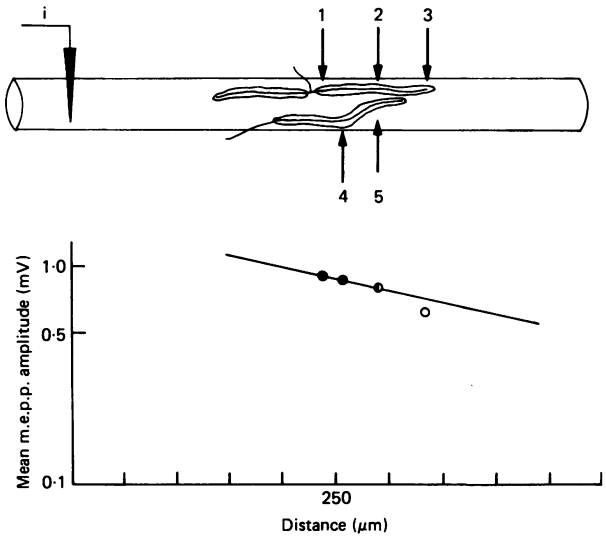

Fig. 5. Camera lucida drawing of an axon and ChE-stained neuromuscular junction. Nerve terminal branches originating from two different axon collaterals are visible. Arrows: sites of extracellular electrode positions; i: intracellular electrode. Numbers indicate the sequence of recordings. In the semilogarithmic plot below mean m.e.p.p. amplitudes from positions 1, 2, 4 and 5 fall on a single straight line, at 2 and 5 identical values were obtained (◐). At 3 (distal end of axon terminal) a lower-than-expected value was found (○), and this point was excluded from the analysis.

the quantum size at the other branches varied (spots 6 and 7). Thus, for calculating the regression line only spots located on a single nerve branch (spots 1/5, 2 and 3 in Fig. 6) could be used.

Consequently, for establishing a typical quantum size the procedure followed in all experiments was to eliminate – irrespective of the actual mean m.e.p.p. amplitude – each spot which after staining turned out to be located at one of the singularities defined above, i.e. ChE rings and distal ends of nerve terminal branches. From the remaining sites those located at one and the same nerve terminal branch (called reference branch hereafter) were used to calculate a new regression line. Since a minimum of three points on the reference branch was needed to calculate a regression line, only fifteen experiments from a total of thirty could be used for the final evaluation. The results are summarized in Fig. 7. The basic idea was to compare for each point the deviation from the over-all regression line with the deviation from the corresponding new regression line. The column marked A (Fig. 7) shows the relative deviations from the over-all regression lines for all points in the fifteen experiments selected (see above); the next four columns (R, DE, B and RS) indicate the relative deviations from the new regression lines in these experiments. Mean m.e.p.p. amplitudes collected from a ChE ring (R), the distal end of a branch (DE) or a spot not located on the reference branch (B) deviate in twenty-five out of thirty-one cases by more than 10%. The remaining fifty-nine points (RS) (i.e. the points which were used to calculate the new regression lines) deviate by less than 10%. This scatter is clearly smaller than at A and compares favourably with the scatter obtained in control measurements (a, b in Fig. 7 and upper histogram in Fig. 2).

These results indicate that while many spots on a single nerve terminal branch have

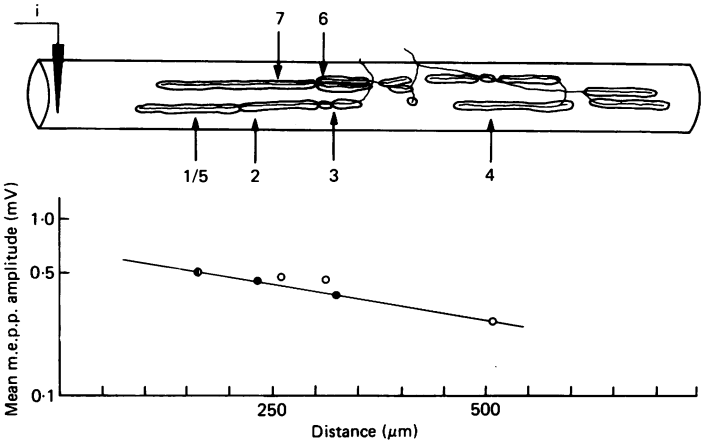

Fig. 6. Camera lucida drawing of a frog neuromuscular junction with positions of the focal (1–7) and the intracellular (i) electrodes. Cell diameter: 75 μm. The regression line in the semilogarithmic plot was calculated from the values obtained at a single branch (1/5, 2 and 3). Mean m.e.p.p. amplitudes obtained from recording 1 and 5 were almost identical (◐). Values from positions 4, 6 and 7 are represented by ○.

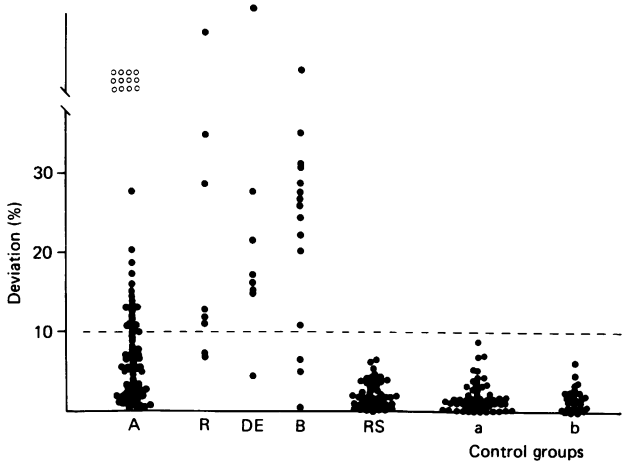

Fig. 7. Relative deviations of mean quantum amplitudes from the over-all regression lines (A) and from the new regression lines (R, DE, B, RS). The latter are split according to the following morphological criteria: spots at ChE rings (R), distal ends of nerve terminal branches (DE), other than the reference branch (B) and the remaining spots (RS). Also included are two control groups, a: repeat recordings from identical spots and b: repeat recordings after moving the electrode laterally by 1–2 μm. The twelve open circles in column A indicate the number of points from those two experiments in which the over-all regression lines had a positive slope; for these points only deviations from the new regression lines were calculated.

the same quantum size, spots at ChE rings and at distal nerve ends deviate from these values. Spots at different nerve branches (B) deviate in both directions from the typical quantum size with about the same frequency (Fig. 8). In contrast, all spots at ChE rings (R) have larger quanta and all spots at distal ends (DE) have smaller quanta than at the reference spots (Fig. 8).

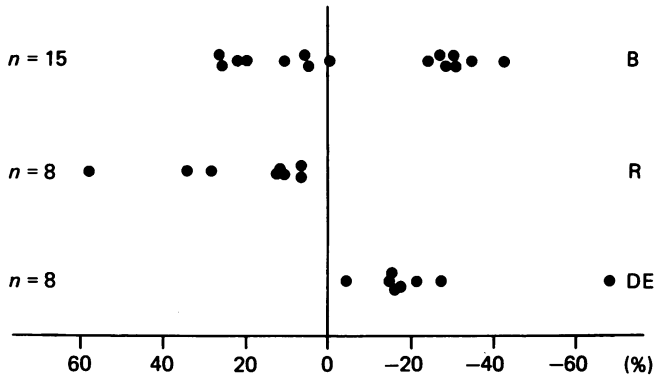

Fig. 8. Directions of mean m.e.p.p. amplitude deviations from the new regression lines (cf. Fig. 7); DE: distal end of a nerve terminal branch, R: ChE ring, B: spots other than the reference branch. At R mean amplitudes are regularly larger and at DE regularly smaller than at the reference branch; at B deviations go in both directions.

Determination of the length constant (λ)

Monitoring quanta discharged at different distances from the intracellular electrode allows one to calculate the muscle fibre's length constant. For this purpose the hypothetical mean quantum amplitude (v_0) at the site of the recording electrode was extrapolated from plots of the mean quantum amplitude *versus* distance from the intracellular electrode (see above). The product $v_0 . 1/e$ was calculated for each plot and λ was determined according to the slope of the regression line. In Fig. 9*B* the resulting value for λ is plotted against the measured fibre diameter. In fifteen muscle fibres with diameters between 30 and 130 μm, values for λ range from about 150 to about 1000 μm. This is in the range expected for fast current signals (Katz & Miledi, 1968; Gage & McBurney, 1972, 1973; Steinbach & Stevens, 1976). As expected for the d.c. length constant (Fatt & Katz, 1951), the m.e.p.p. length constant calculated here also increases with increasing fibre diameter (see Discussion).

For comparison (Fig. 9*A*), λ was determined for the same experiments using the over-all regression lines (which were calculated before elimination of spots at morphological singularities, see above). There is no correspondence between fibre diameter and λ; this and the clear deviation of the three points to the right indicate that over-all regression lines do not provide correct values for fibre length constants.

DISCUSSION

Apart from considerations regarding the sampling technique, the clear deviations of the quantum amplitudes at certain spots and the values obtained for the fibre length constant deserve further discussion.

The sampling technique is a critical factor in comparing mean m.e.p.p. amplitudes at different spots. Differences could arise from different degrees of pressure imposed on the nerve terminal (cf. Katz & Miledi, 1973), the presence of connective tissue plugging the electrode tip and the geometry of the opening of the synaptic cleft. Our control experiments with repeated recordings, including lateral shifts of the electrode, indicate that such factors would account for amplitude shifts of less than 10%.

It is clear that there is some distance on both sides of the focal electrode at which large quanta will be sampled, but not small ones (cf. Wernig, 1976). As long as these distances are about equal at different spots, mean m.e.p.p. amplitudes collected from these spots should be comparable. While this ought to be the case for the junctional portions with apparently continuous synaptic contacts (i.e. continuous double lines of ChE reaction product) and comparable gutter widths (see below), a sampling effect cannot be excluded for spots at, for example, the distal ends of nerve terminal branches. The lower mean quantum amplitudes consistently observed here could be

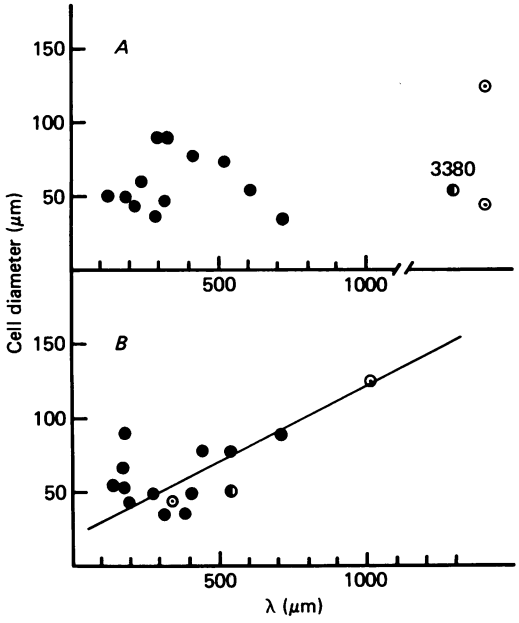

Fig. 9. Relationship between fibre diameter (measured) and m.e.p.p. length constant (λ) for the remaining fifteen experiments. In the upper plot (*A*), λ was determined from the over-all regression line (i.e. including all recordings at a neuromuscular junction). Note that in two experiments no length constant could be determined (⊙) and one experiment had an unrealistic length constant of 3380 μm (◐). In the lower plot (*B*), λ was determined from the new regression lines. In this plot there is some correspondence between fibre diameter and λ. The line was fitted by eye. Same symbols for identical experiments in *A* and *B*.

due to the asymmetric and reduced sampling of larger quanta at the nerve end. The larger mean m.e.p.p. amplitudes observed at ChE rings cannot be explained by sampling effects: the presumed loss of large quanta from distant regions (see above) would tend to decrease rather than to increase mean amplitudes. Also, as appears from ultrastructural observations (Anzil *et al.* 1984), the extracellular space between muscle fibre and axon-surrounding Schwann cell is considerably larger immediately outside a ChE ring than at the synaptic cleft. Consequently, the extracellular length constant at such regions is much smaller and electrical events at distant release sites are unlikely to be monitored at the ChE ring.

Apart from distal nerve ends and ChE rings, quantum amplitudes were remarkably similar at different spots along a single nerve terminal branch. Among different nerve

terminal branches in a single junction, quantum amplitudes were similar in several cases but deviated in others. To explain this discrepancy it is conceivable that the extracellular length constant also depends on the width of the synaptic gutter occupied by nerve and thus on the actual axon diameter. Judging from silver-stained preparations, axon diameters do not change over long distances along a single nerve terminal branch while they can vary markedly when different nerve terminal branches are compared within a single junction (Wernig *et al.* 1980*a*, *b*). Without any experimental evidence that this notion applies here, the different quantum amplitudes observed at different nerve terminal branches could thus be due to different sampling characteristics at differently sized terminal branches.

The larger mean quantum amplitudes collected at ChE rings are not easy to understand. At some ChE rings newly formed contacts have been observed, but contacts seemed mature at other ChE rings (Anzil *et al.* 1984). Thus a variety of factors determining quantum amplitudes including ChE activity, receptor density and transmitter diffusion pathways in the cleft, can all be different at different ChE rings. What new contacts have in common is a markedly reduced complexity of the opposing post-synaptic membrane; this is either due to the missing or poor development of secondary folds or, in any case due to the absence of secondary folds on either side of ChE rings. All this tends to reduce the capacitance of the muscle fibre membrane around the current source as compared to other portions of the junction. If the decrease in capacitance is effective at all it would be bound to increase m.e.p.p. amplitudes (cf. Gage & McBurney, 1973); whether this factor is sufficient to account for the observed larger quantum amplitudes is somewhat hard to estimate without further experimentation.

Another point which deserves further consideration is the low values obtained for λ. Values for λ obtained from d.c. measurements (λ_0) amount to about 2000 μm for fibres with 75 μm diameter (Katz, 1966). When using the equation derived by Katz & Miledi (1968) for alternating currents, λ_f (the length constant for sinusoidal currents of frequency f) reduces to values comparable to those observed here (see also Steinbach & Stevens, 1976). For example, assuming a synaptic current frequency (f) of 1250 Hz and $\lambda_0 = 2000$ μm, the equation

$$\lambda_f = \lambda_0 \cdot \sqrt{\frac{2}{1+\sqrt{(1+4\pi^2 f^2 \tau^2)}}} \quad \text{(Katz \& Miledi, 1968)},$$

gives a value of 210 μm. τ (membrane time constant) was assumed to be 23 ms (Katz, 1966). For larger muscle fibres the correspondence with our measurements becomes worse however. Assuming a fibre diameter of 130 μm and $\lambda_0 = 2550$ μm (from $\lambda_0 = \sqrt{(r/2 \cdot R_m/R_i)}$, r = fibre radius, R_m (specific membrane resistance) = 4000 Ω cm^2, R_i (specific resistance of cell interior) = 200 Ω cm; Fatt & Katz, 1951; Katz, 1966), λ_f (calculated) would then be 267 μm while we find a length constant of about 1000 μm. At the present time we cannot resolve this discrepancy.

This work was supported by the Deutsche Forschungsgemeinschaft (We 859). Initial experiments were performed at the Max Planck Institute for Psychiatry, München. We want to thank Dr Brian Freeman for critical reading and correcting the manuscript.

REFERENCES

ANZIL, A. P., BIESER, A. & WERNIG, A. (1984). Light and electron microscopic identification of nerve terminal sprouting and retraction in normal adult frog muscle. *J. Physiol.* **350**, 393–399.

BIESER, A. & WERNIG, A. (1982). Inhomogeneity of quantum size in normal frog neuromuscular junctions. *Pflügers Arch.* **394**, suppl. R 51.

FATT, P. & KATZ, B. (1951). An analysis of the end-plate potential recorded with an intra-cellular electrode. *J. Physiol.* **115**, 320–370.

GAGE, P. W. & MCBURNEY, R. N. (1972). Miniature end-plate currents and potentials generated by quanta of acetylcholine in glycerol-treated toad sartorius fibres. *J. Physiol.* **226**, 79–94.

GAGE, P. W. & MCBURNEY, R. N. (1973). An analysis of the relationship between the current and potential generated by a quantum of acetylcholine in muscle fibers without transverse tubules. *J. Membrane Biol.* **12**, 247–277.

KATZ, B. (1966). *Nerve, Muscle and Synapse.* London: McGraw-Hill.

KATZ, B. & MILEDI, R. (1968). The effect of local blockage of motor nerve terminals. *J. Physiol.* **199**, 729–741.

KATZ, B. & MILEDI, R. (1973). The binding of acetylcholine to receptors and its removal from the synaptic cleft. *J. Physiol.* **231**, 549–557.

MARTIN, A. R. (1955). A further study of the statistical composition of the end-plate potential. *J. Physiol.* **130**, 114–122.

MCLACHLAN, E. M. & MARTIN, A. R. (1981). Non-linear summation of end-plate potentials in the frog and mouse. *J. Physiol.* **311**, 307–324.

PÉCOT-DECHAVASSINE, M., WERNIG, A. & STÖVER, H. (1979). A combined silver and cholinesterase method for studying exact relations between the pre- and the postsynaptic elements at the frog neuromuscular junction. *Stain Technol.* **54**, 25–28.

STEINBACH, J. H. & STEVENS, C. F. (1976). Neuromuscular Transmission. In *Frog Neurobiology*, ed. LLINÁS, R. & PRECHT, W., pp. 33–92. Berlin: Springer.

WERNIG, A. (1976). Localization of active sites in the neuromuscular junction of the frog. *Brain Res.* **118**, 63–72.

WERNIG, A., PÉCOT-DECHAVASSINE, M. & STÖVER, H. (1980*a*). Sprouting and regression of the nerve at the frog neuromuscular junction in normal conditions and after prolonged paralysis with curare. *J. Neurocytol.* **9**, 277–303.

WERNIG, A., PÉCOT-DECHAVASSINE, M. & STÖVER, H. (1980*b*). Signs of nerve regression and sprouting in the frog neuromuscular synapse. In *Ontogenesis and Functional Mechanisms of Peripheral Synapses*, ed. TAXI, J., pp. 225–238. Amsterdam: Elsevier/North Holland Biomedical Press.